# Phase Behavior of Ternary Homopolymer/Gradient Copolymer Blends

**Rui Wang,[†,‡] Weihua Li,[‡] Yingwu Luo,[†] Bo-Geng Li,*[,†] An-Chang Shi,*[,‡] and Shiping Zhu*[,§]**

*Department of Chemical & Biochemical Engineering, State Key Laboratory of Polymer Reaction Engineering, Zhejiang University, Hangzhou, Zhejiang, P.R. China 310017; Department of Physics and Astronomy, McMaster University, Hamilton, Ontario, Canada L8S 4L7; and Department of Chemical Engineering, McMaster University, Hamilton, Ontario, Canada L8S 4L7*

*Received June 22, 2008; Revised Manuscript Received February 2, 2009*

ABSTRACT: The phase behavior of ternary homopolymer/gradient copolymer blends is studied theoretically using a multiblock model of gradient copolymers. Critical lines and Lifshitz points of the blends are determined by a random phase approximation analysis. Phase diagrams and microphase structures of the blends are studied using self-consistent mean-field theory. It is discovered that the chain gradient distribution has a significant effect on the phase behavior of the blends. When the chain gradient distribution is gradual, a larger amount of copolymers and a higher incompatibility are needed for the formation of a microphase. In addition, the ability of copolymer domains to absorb homopolymers decreases, whereas the solubility of copolymers in homopolymer matrix increases, as the gradient distribution becomes gradual. Another important effect is that gradient copolymers lead to a broad interface between two incompatible polymers. These results indicate that interfacial structure and morphology of these blends can be fine-tuned by specifically designed gradient distributions.

## Introduction

New and/or improved physical and chemical properties of polymeric materials can often be obtained by mixing different types of polymers to form polymer blends.[1,2] The properties of polymer blends are mainly determined by the dispersion and morphology of polymer domains as well as the properties of the interfaces between the different polymer domains. Because of the incompatibility of the homopolymers (A and B), phase separation at a macroscopic scale tends to occur. In order to increase the miscibility and to control the dispersion, block or graft copolymers composed of A- and B-type monomers are often employed as compatibilizers.[3,4] When a small amount of AB copolymer is added to an A/B blend, the copolymers tend to segregate to the A/B interfaces to screen unfavorable contacts between A and B. The reduced interfacial tension leads to the formation of small droplets at a micrometer scale. Block copolymers at the interfaces can also provide steric and hydrodynamic repulsion to suppress coalescence. A combination of these two effects leads to improved dispersion of the minority polymer component. In addition, the stitching of copolymers into homopolymer layers could significantly strengthen fragile interfaces.[5] For a small amount of added copolymers, the dispersion is thermodynamically unstable, although it may last over a time scale encountered in most polymer processing cycles. When the volume fraction of copolymers in the blend increases, the dispersion size shrinks to tens of nanometers and becomes thermodynamically stable. In this case, AB block copolymers can self-assemble into various ordered microstructures,[6] which can become a template to structure the blends. The homopolymers would serve as filler materials that are used to adjust the curvature of the morphology. Various intriguing morphologies are obtained by changing the copolymer architecture and the blend recipe. An interesting example is the polymeric microemulsion from ternary homopolymer/block copolymer blends obtained by Bates and co-workers.[7−9] This bicontinuous morphology, located within a narrow channel near the theoretical Lifshitz point, could have a large impact on diverse properties such as electrical or ionic conductivity, permeability, elasticity, etc. The importance of this line of research motivated Ruzette and Leibler to suggest that nanostuctured polymer blends stand for a trend in future plastics.[10]

The phase behavior of homopolymer/copolymer blends is controlled by many parameters, including monomer−monomer interactions, chain lengths, and copolymer architectures. Therefore, the parameter space of the blends is extremely large. Exploring the phase behavior of homopolymer/copolymer blends is, therefore, a challenging task. To this end, it is desirable to develop theoretical methodologies that are capable of describing and predicting the different morphologies and phase transitions in this complex system.[11,12] Over the past two decades, the theory of microphase separation of block copolymers has been well developed, ranging from analytical approximate descriptions in the weak[13] or strong[14−16] segregation region to sophisticated numerical solutions within the framework of self-consistent-field theory (SCFT).[17−21] For the case of polymer blends, Broseta and Fredrickson used the Flory−Huggins free energy and random phase approximation to investigate critical phenomena in ternary blends of A, B homopolymers and AB diblock copolymers.[22] In particular, they located an isotropic Lifshitz point (LP)[23] in the blends and studied the effect of the chain length ratio of the homopolymer to the copolymer on the LP. In addition, several theoretical methods have been used to calculate the phase diagrams of homopolymer/diblock copolymer blends. Using Monte Carlo simulations, Mueller and Schick observed a coexistence region between two homopolymer-rich phases and a spatially structured, copolymer-rich phase in ternary homopolymer/diblock copolymer blends.[24] Furthermore, Janert and Schick, as well as Matsen, have made noticeable efforts to apply the SCFT to binary and ternary blends.[25−30] Using SCFT calculations, Janert and Schick predicted full phase diagrams of ternary A/B/AB blends, which contain a continuous unbinding transition from lamellae to homopolymer-rich phases.[28] In a later study Matsen pointed out that this transition could be first order, based on a more accurate calculation.[27]

* To whom correspondence should be addressed: e-mail bgli@zju.edu.cn, Tel 86-571-87952623, Fax 86-571-87951612 (B.-G.L); e-mail shi@macmaster.ca, Tel (905)525-9140ext 24060, Fax (905)521-2773 (A.-C.S.); e-mail zhuship@macmaster.ca, Tel (905)525-9140ext 24962, Fax (905)521-1350 (S.Z.).

[†] Zhejiang University.

[‡] Department of Physics and Astronomy, McMaster University.

[§] Department of Chemical Engineering, McMaster University.

10.1021/ma801398a CCC: $40.75 
Published on Web 02/25/2009

Recently, Duchs et al. applied a general field-theoretic simulation to study the effect of fluctuations on the blends.[31] Besides these previous studies on the phase behavior of the blends, a number of investigations have been carried out, focusing on interfacial properties such as density profiles, interfacial tension, critical micelle concentration, and elastic modulus.[32−34] These previous theoretical studies provided valuable guidance for the design and optimization of ternary polymer blends.

It is well-known that the structure of copolymers is a key factor that affects the dispersion of polymer blends. It has been argued previously that micellization of block and graft copolymers prevents their transport from homopolymer bulk phases to the interfaces, thus limiting the efficiency of these copolymers as compatibilizers.[35] On the other hand, random copolymers do not possess a strong driving force to segregate to the interfaces; thus, they usually do not form microphases as structured nanoblends.[36] Recently, progress in living radical polymerization has led to the synthesis of a new class of copolymers, the so-called gradient copolymers.[37−39] Gradient copolymers exhibit intermediate chain architectures between block and random copolymers. In a gradient copolymer, the composition of monomers along the chain changes continuously. This is different from the usual block copolymer, in which the composition distribution along the chain is a step function, and random copolymers, in which the composition distribution is a constant. Instead, the composition of an AB gradient copolymer changes gradually along the chain from A-rich at one end to B-rich at the other end. What makes the gradient copolymers interesting is that this composition distribution can be tailored using a number of different strategies.[40,41] Recently our group has launched a research program on the development of reactor technologies for the design and control of optimal gradient copolymer products.[42−45] Using semibatch feeding policies, we obtained gradient copolymers with various composition profiles, such as uniform, diblock, linear, and tanh gradients.

Physical properties of gradient copolymers have been investigated in a number of previous studies. Jouenne et al. and Hodrokoukes et al. observed that some types of gradient copolymers can form microphases, similar to block copolymers but at lower temperatures.[46,47] In addition, several research groups found a uniquely broad glass transition temperature in gradient copolymers.[41,43,48] Furthermore, Kim et al. experimentally demonstrated that gradient copolymers have special interfacial properties in immiscible blends, providing an intriguing route to design new compatibilizers.[49,50] The properties of gradient copolymers have also attracted considerable theoretical attention. Aksimentiev and Holyst have studied the phase properties of different gradient copolymer melts using a Ginzburg−Landau theory.[51] Different scenarios of phase transformations in gradient copolymer systems have been proposed. Lefebvre et al. located the critical points for different types of gradient copolymers using the random phase approximation (RPA) and investigated the effect of chain gradients on the period and density profile of lamellar phases by solving an approximate SCFT model.[52] Shull studied the interfacial behavior of gradient copolymers in immiscible polymer blends.[53] Very recently, Jiang et al. developed a multiblock model for gradient copolymers.[54] Implementation of the multiblock model to SCFT in reciprocal space allowed them to construct full mean-field phase diagrams for gradient copolymer melts. These previous studies provide a good understanding of the self-assembly behavior of gradient copolymer melts. However, to the best of our knowledge, the phase behavior of homopolymer/gradient copolymer blends has not been investigated.

In this paper, we report our study of the critical behavior, phase diagrams, and mesophase structures of ternary homopolymer/gradient copolymer blends. The phase behavior of blends containing A/B homopolymers and AB gradient copolymers is controlled by a large number of parameters, including the molecular weights of the polymers and the composition of the blend. In the current study, we focus on the symmetric case, in which the two homopolymers have the same chain length and volume fraction in the blends. The average composition of the gradient copolymers is also restricted to be symmetric. Following Jiang and co-workers,[54] a multiblock model is employed to describe the composition profiles of the gradient copolymers. For the model blends, critical lines and Lifshitz points as a function of the gradient distribution are determined using random phase approximation (RPA) analysis.[55] The nature of the Lifshitz points and their dependence on the chain length ratio between the copolymers and homopolymers are also elucidated. Furthermore, phase diagrams of the symmetric ternary blends with a series of gradient copolymers are constructed by solving the SCFT equations using a pseudospectral approach.[56,57] Finally, microstructures of the lamellar phases are investigated. The effects of chain gradient distribution on the density profiles of the copolymers and homopolymers in the blends are analyzed.

## Theoretical Framework

**Description of Gradient Distributions.** From the perspective of living polymerization, the growth of a copolymer chain is a Markov process.[58] The copolymer composition and sequence distribution are determined by two factors. One is the instantaneous comonomer composition, $f$, whereas the other is the matrix of transition probabilities, $P$, whose elements $P_{ij}$ represent the conditional probability of a type-$i$ unit at an arbitrary position in the chain followed immediately by the growth of a type-$j$ unit. The parameters $f$ and $P_{ij}$ change gradually during the polymerization process, resulting in "composition drifting" and the formation of gradient copolymers. The composition profile of gradient copolymers can be formed spontaneously in batch reactors, or it can be controlled by semibatch processes. Because of their statistical nature, gradient copolymers present quenched random systems. That is, for a given length of segment along the chain, there is a composition distribution among different chains. We use $F_i(s,\Delta s)$ to denote the composition of a segment located at position $s$ of the $i$th chain with the length $\Delta s$. The average composition at position $s$ is

$$F(s,\Delta s) = \frac{1}{n}\sum_i F_i(s,\Delta s) \tag{1}$$

where $n$ is the total number of polymer chains. Therefore, a gradient copolymer is a random copolymer with a specific average composition distribution, $F(s,\Delta s)$, along the chain backbone.

In principle, gradient copolymers should be described using a statistical ensemble, in which each polymer chain is randomly sampled from a specific distribution. Although the statistical nature of gradient copolymers is an important feature, most of the theoretical treatments of gradient copolymers employ a simple coarse-grained method, in which all polymer chains are assumed to have the same composition profile, $F(s,\Delta s)$. Furthermore, a continuous function, $g(s)$, is used to describe the local composition density:

$$g(s) = \left(\frac{\partial F(s,\Delta s)}{\partial(\Delta s)}\right)\Bigg|_{\Delta s=0} \quad \text{or} \quad F(s,\Delta s) = \frac{1}{\Delta s}\int_s^{s+\Delta s} g(t)\,\mathrm{d}t \tag{2}$$

This continuous model with a specific $g(s)$ provides a convenient way to describe the composition profile of chain gradients. For example, an ideal random copolymer corresponds to $g(s)$ being

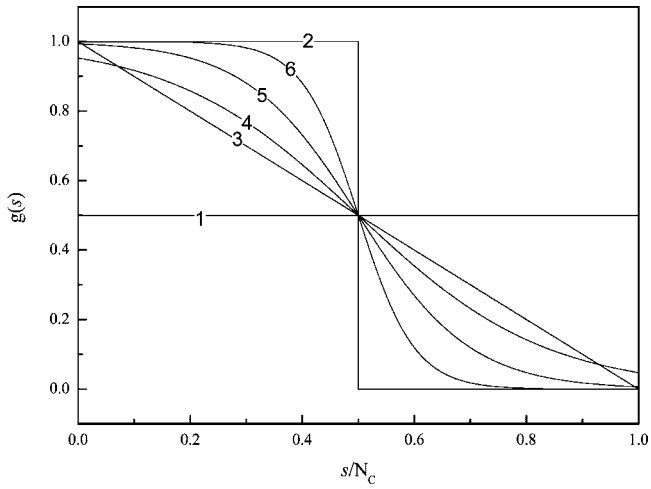


**Figure 1.** Composition profiles of gradient copolymers. Lines 1−6 represent uniform, diblock, linear, and three tanh ($\lambda$ = 3, 5, and 10) gradient copolymers, respectively.

a constant function ("uniform" gradient copolymer), whereas a diblock copolymer corresponds to a step function. For the symmetric diblock copolymers the distribution function is given by

$$g(s) = \begin{cases} 1 & s < N_c/2 \\ 0 & s > N_c/2 \end{cases} \tag{3a}$$

where $N_c$ is the chain length of copolymers. Another example is so-called "linear gradient" copolymer which is specified by the distribution function

$$g(s) = \frac{1}{N_c} s \tag{3b}$$

An important class of gradient copolymers is the so-called "tanh gradient" copolymers. For this class of gradient copolymers the distribution function $g(s)$ is a hyperbolic tangent function

$$g(s) = \frac{1}{2}\left[1 - \tanh\left(\lambda\left(\frac{s}{N_c} - \frac{1}{2}\right)\right)\right] \tag{3c}$$

where $\lambda$ is an adjustable parameter which determines the steepness of the composition profiles. When $\lambda$ is increased, the tanh gradient copolymer changes from linearlike to blocklike, as illustrated in Figure 1.

In the continuous model, the copolymer composition in the interval between $s$ and $s + ds$ is neither A nor B, but a combination of $g(s)$ A monomers and $(1 - g(s))$ B monomers. This ambiguity makes it difficulty to implement the self-consistent mean-field theory in reciprocal space. As an alterative to the continuous gradient distributions, Jiang and co-workers have proposed a multiblock model for gradient copolymers.[52] In the multiblock model, a copolymer chain is divided into certain number of intervals. Each interval is assumed to be an AB diblock copolymer, whose composition (A monomer ratio) is specified by the local gradient distribution function $g(s)$. Thus, the local composition density in an interval $[s, s + \Delta s]$ is no longer continuous but a step function specified by the following equation:

$$f(t) = \begin{cases} 1 & s < t < s + F(s, \Delta s)\Delta s \\ 0 & s + F(s, \Delta s)\Delta s < t < s + \Delta s \end{cases} \tag{4}$$

Jiang et al. have validated the applicability of the multiblock model to gradient copolymers, and they have shown that the multiblock model gives a good description of the phase behavior of gradient copolymers.[54] The advantage of the multiblock model is that the SCFT can be implemented straightforwardly. Therefore, we can apply available SCFT techniques to study the properties and phase behavior of a gradient copolymer. In what follows we will employ the multiblock model in our study of homopolymer/gradient copolymer blends. Similar to the previous work of Jiang et al., the gradient copolymer chains are divided into $X$ intervals of identical lengths, $\Delta s = N_C/X$. The $i$th interval ($i$ = 0, 1, 2,..., $X$ − 1) starts with an A block in the range $[i\Delta s, (i + F_i)\Delta s]$, followed by a B block in the range $[(i + F_i)\Delta s, (i + 1)\Delta s]$, where $F_i$ is the fraction of A blocks for the $i$th interval. For a given gradient distribution function $g(s)$, the fraction $F_i$ is given by

$$F_i = X\int_{i/X}^{(i+1)/X} g(s)\, ds \tag{5}$$

**Homogeneous Phases.** We assume that the interaction between the A and B monomers is described by the usual Flory−Huggins parameter $\chi$. The miscibility of a symmetric AB homopolymer blend is characterized by the product $\chi N$, where $N = N_A = N_B$ is the degree of polymerization of the homopolymers. For small values of $\chi N$, the A and B polymers in the blend are miscible, leading to a homogeneous state. In the homogeneous phase the concentration of the polymers, $\phi_K(\mathbf{r})$, is a constant which is independent of the spatial position. For $\chi N$ larger than a critical value, the homogeneous phase becomes unstable against concentration fluctuations $\delta\phi(\mathbf{r})$, leading to phase separation of the two homopolymers. The critical behaviors may be of two types, macroscopic or microscopic separation. For homopolymer blends, macroscopic phase separation occurs at large incompatibility ($\chi N > 2$ for the symmetric binary blends). For macroscopic phase separation, the structure factor diverges at a wave vector $q^* = 0$ when the system is approaching the critical point. In contrast, block copolymers and gradient copolymers may undergo microscopic phase separation into spatially modulated phases at high $\chi N$. For example, mean-field theory predicts that a lamellar phase is formed when $\chi N > 10.5$ for symmetric diblock copolymers[13] or when $\chi N > 29.3$ for linear gradient copolymers.[52] A signature of the microscopic phase separation is that the structure factor shows a peak at a nonzero wave vector ($q^* \neq 0$) even in the disorder state. This peak becomes singular at the critical point. For the symmetric gradient copolymer/homopolymer blends considered in this paper, both of these two critical behaviors can occur. When the fraction of gradient copolymers is increased in the blends, the phase separation is macroscopic at first and changes to microscopic at higher gradient copolymer contents. The point at which the macroscopic phase separation changes to microscopic phase separation is called the Lifshitz point (LP).[22,23] At the neighborhood of this point, $q^*$ increases continuously from zero to a positive value.

The critical line as well as the LP can be determined using the random-phase approximation (RPA), which was introduced into polymer physics by de Gennes.[56] Over the past 30 years, RPA has been broadly employed to describe the behavior of homogeneous polymer systems. In the RPA the structure factor, $S(q)$, which is defined as the correlation function of the concentration fluctuations, $S(q) = \langle\delta\phi_A(q)\delta\phi_A(-q)\rangle = \langle\delta\phi_B(q)\delta\phi_B(-q)\rangle$, can be calculated in terms of the structure factors of noninteracting Gaussian chains

$$S^{-1}(q) = \frac{\sum_{i,j} S_{ij}(q)}{\det \mathbf{S}} - 2\chi \tag{6}$$

where $S_{ij}(q)$ are correlation functions of unit $i$ and unit $j$ in a noninteracting system, and $\mathbf{S}$ is the matrix formed by $S_{ij}(q)$. The

correlation functions, $S_{ij}(q)$, contain contributions from the homopolymers and the copolymers, $S_{AA}(q) = \phi_{hA}S^{h}_{AA}(q) + \phi_c S^{c}_{AA}(q)$, $S_{BB}(q) = \phi_{hB}S^{h}_{BB}(q) + \phi_c S^{c}_{BB}(q)$, and $S_{AB}(q) = \phi_c S^{c}_{AB}$, where $\phi_{hA}$, $\phi_{hB}$, and $\phi_c$ are the volume fractions of homopolymer A, B, and the copolymer, respectively. $S^{h}_{AA}$ and $S^{h}_{BB}$ are the single-chain correlation functions of the homopolymers A and B, respectively. These correlation functions have been calculated as $S^{h}_{AA}(q) = N_{hA}g_h(x_{hA})$ and $S^{h}_{BB}(q) = N_{hB}g_h(x_{hB})$, where $N_{hA} = \alpha_A N_c$ and $N_{hB} = \alpha_B N_c$ are the chain lengths of homopolymers A and B, $x_{hA}$ and $x_{hB}$ are the scattering wavenumbers defined by $x_{hA} = N_{hA}b^2q^2/6 = \alpha_A R_{g,c}{}^2q^2$, and $x_{hB} = N_{hB}b^2q^2/6 = \alpha_B R_{g,c}{}^2q^2$ ($b$ is the statistical unit length, taken to be the same for both monomers, and $R_{g,c}$ is the gyration radius of the copolymer chain). Finally, $g_h(x)$ is the Debye function, $g_h(x) = 2(x + e^{-x} - 1)/x^2$. Moreover, the calculation for the single-chain correlation functions of the gradient copolymers, $S^{c}_{AA}$, $S^{c}_{AB}$, and $S^{c}_{BB}$, depends on the model used to describe the chain gradient. For the multiblock model, these correlation functions are given by

$$S^{c}_{AA}(q) = N_c \sum_{i=0}^{X-1}\sum_{j=0}^{X-1} \int_{j/X}^{(j+F_j)/X} \int_{i/X}^{(i+F_i)/X} \exp(-x_c|t - t'|)\, dt\, dt' = N_c g_{AA}(x_c) \quad (7a)$$

$$S^{c}_{BB}(q) = N_c \sum_{0}^{X-1}\sum_{0}^{X-1} \int_{(j+F_j)/X}^{(j+1)/X} \int_{(i+F_i)/X}^{(i+1)/X} \exp(-x_c|t - t'|)\, dt\, dt' = N_c g_{BB}(x_c) \quad (7b)$$

$$S^{c}_{AB}(q) = N_c \sum_{0}^{X-1}\sum_{0}^{X-1} \int_{(j+F_j)/X}^{(j+1)/X} \int_{i/X}^{(i+F_i)/X} \exp(-x_c|t - t'|)\, dt\, dt' = N_c g_{AB}(x_c) \quad (7c)$$

In our calculations, the contour length of each gradient copolymer chain is divided into 256 intervals ($X = 256$). The complete set of RPA equations (eqs 6 and 7) can be used to describe any ternary gradient copolymer/homopolymer blends. For the symmetric blends, the two homopolymers are of equal lengths and equal volume fractions in the blend formulation (i.e., $\alpha_A = \alpha_B = \alpha$ and $\phi_{hA} = \phi_{hB} = (1 - \phi_c)/2$). Furthermore, the gradient copolymers are assumed to be symmetric in composition (i.e., $g_{AA}(x_c) = g_{BB}(x_c)$). For the symmetric blends, the structure factor can be simplified as

$$S^{-1}(q) = \frac{F(x_c)}{N_c} - 2\chi \quad (8)$$

where $F(x_c) = [\alpha(1 - \phi_c)g_h(\alpha x_c) + 2\phi_c(g_{AA}(x_c) + g_{AB}(x_c))]/[(\alpha(1 - \phi_c)g_h(\alpha x_c)/2 + \phi_c g_{AA}(x_c))^2 - (\phi_c g_{AB}(x_c))^2]$. For fixed values of copolymer content, $\phi_c$, and chain length ratio, $\alpha$, the characteristic scattering wavenumber, $x_c^*$, is the one which minimizes the function $F(x_c)$. The critical point, $(\chi N_c)_c$, can then be simply computed from eq 8 as $F(x_c^*)/2$. When $\chi N$ is increased to $(\chi N_c)_c$, the structure factor diverges, and the system reaches a spinodal point. The critical line can then be obtained by tracking the value of $(\chi N_c)_c$ as a function of $\phi_c$. The value of the critical wavevector, $x_c^*$, determines the natural period of the phase transition. When $x_c^*$ equals zero, the phase transition corresponds to macroscopic phase separation. On the other hand, when $x_c^*$ is nonzero, a length scale is selected and the phase transition corresponds to microscopic phase separation, leading to the formation of periodically modulated structures. In general, $x_c^*$ is a function of the polymer concentration $x_c^* = x_c^*(\phi_c)$, and the LP is located at the specific value of $\phi_c$ at which $x_c^*(\phi_c)$ becomes nonzero.

**Inhomogeneous Region.** For large values of AB interactions, $\chi N_c > (\chi N_c)_c$, the polymer blend is in the phase-separated region, resulting in an inhomogeneous phase. The properties of an inhomogeneous polymer blend can be described using the self-consistent-field theory. For a multicomponent polymeric system, the best framework is the self-consistent-field theory formulated in grand canonical ensemble. In a grand canonical ensemble, the chemical potentials, $\mu_K$ ($K$ = A, B, AB), of each component are used as the controlling parameters, whereas the numbers of the polymer chains, $n_K$, are determined from the chemical potentials. The ternary blend is assumed to be incompressible, and each monomer has the same volume, $1/\rho_0$. The polymer chains are modeled as flexible Gaussian chains. The interactions between the different components are modeled using the standard Flory−Huggins interactions. Within the self-consistent formulation, the grand partition function of the blend is given by $Z \propto \int \mathcal{D}\Phi_A \mathcal{D}\Phi_B \mathcal{D}W_A \mathcal{D}W_B \mathcal{D}\Xi \exp[-\beta F(\Phi_A,\Phi_B,W_A,W_B,\Xi)]$, where $\Phi_K$ ($K$ = A or B) are composition densities and $W_K$ are corresponding conjugate fields for monomer $K$. The function $\Xi$ is a Lagrange multiplier to ensure the incompressibility condition. The free energy functional is given by the expression

$$N_c F\beta/\rho_0 = -z_A Q_A - z_B Q_B - Q_C + \int d\mathbf{r}(\chi N_c \Phi_A \Phi_B - W_A\Phi_A - W_B\Phi_B - \Xi(1 - \Phi_A - \Phi_B)) \quad (9)$$

where $z_K = \exp(\beta\mu_K)$ and $\beta = 1/k_B T$. It should be noticed that the chemical potentials are measured with respect to that of the copolymers. The quantities $Q_K$ are the partition functions of single chain in the external fields. For the homopolymers A or B, $Q_K = \int \mathcal{D}\mathbf{r}_K(s) P[\mathbf{r}_K(s);0,\alpha_K] \exp[-\int_0^{\alpha_K} ds\, W_K(\mathbf{r}_K(s))]$, where $P$ is the Gaussian distribution function for a homopolymer. For the gradient copolymers, the multiblock model of Jiang et al. is employed in our study. Specifically, the monomer distribution along the chain is described by two functions, $\sigma_A(t)$ and $\sigma_B(t)$, corresponding to the gradient distribution of eq 4

$$\sigma_A(t) = \begin{cases} 1 & i/X < t < (i + F_i)/X \\ 0 & (i + F_i)/X < t < (i + 1)/X \end{cases} \quad (10a)$$

$$\sigma_B(t) = 1 - \sigma_A(t) \quad (10b)$$

The partition function of a gradient copolymer is then given by $Q_C = \int \mathcal{D}\mathbf{r}_C(s) P[\mathbf{r}_C(s);0,1] \exp[-\int_0^1 ds \sum_K \sigma_K(s) W_K(\mathbf{r}_C(s))]$.

Within the mean-field approximation, the free energy of the blend is obtained by $F(\phi_A,\phi_B,w_A,w_B,\xi)$, where $\phi_A$, $\phi_B$, $w_A$, $w_B$, and $\xi$ are functions which minimize the free energy functional $F$. The minimization condition leads to the following set of SCFT equations

$$\phi_A = z_A \frac{\delta Q_A}{\delta w_A} + \frac{\delta Q_C}{\delta w_A} \quad (11a)$$

$$\phi_B = z_B \frac{\delta Q_B}{\delta w_B} + \frac{\delta Q_C}{\delta w_B} \quad (11b)$$

$$w_A(\mathbf{r}) = \chi N \phi_B(\mathbf{r}) + \xi(\mathbf{r}) \quad (11c)$$

$$w_B(\mathbf{r}) = \chi N \phi_A(\mathbf{r}) + \xi(\mathbf{r}) \quad (11d)$$

$$\phi_A(\mathbf{r}) + \phi_B(\mathbf{r}) = 1 \quad (11e)$$

For the single chain partition functions, it is convenient to express them in terms of the end-integrated propagators, $Q_K = \int d\mathbf{r}\, q_K(\mathbf{r},\alpha_K)$ ($K$ = A or B) and $Q_C = \int d\mathbf{r}\, q_C(\mathbf{r},1)$. These end-

integrated propagators, $q_K(\mathbf{r},s)$ and $q_C(\mathbf{r},s)$, are solutions to the modified diffusion equations

$$\frac{\partial q_K}{\partial s} = \frac{N_c b^2}{6} q_K - w_K q_K \tag{12a}$$

$$\frac{\partial q_C}{\partial s} = \frac{N_c b^2}{6} q_C - (\sigma_A w_A + \sigma_B w_B) q_C \tag{12b}$$

The initial conditions are $q_K(\mathbf{r},0) = 1$ and $q_C(\mathbf{r},0) = 1$. Furthermore, the monomer densities of the polymers can be expressed in terms of these propagators. For the homopolymers, the densities, $\phi_{hK}(\mathbf{r})$, can be computed by

$$\phi_{hK}(\mathbf{r}) = z_K \int_0^{\alpha_K} \mathrm{d}s\, q_K(\mathbf{r}, s) q_K(\mathbf{r}, \alpha_K - s) \tag{13a}$$

For the gradient copolymers, a complementary chain propagator, $q_C^*(\mathbf{r},s)$, is needed to calculate the monomer density of the copolymers, $\phi_{cK}(\mathbf{r})$. This is due to the fact that the two ends of the copolymers are different. $q_C^*(\mathbf{r},s)$ satisfies eq 12b with the right-hand side multiplied by $-1$ and the initial condition $q_C^*(\mathbf{r},1) = 1$. Using the propagators $q_C(\mathbf{r},s)$ and $q_C^*(\mathbf{r},s)$, the monomer density of the copolymers, $\phi_{cK}(\mathbf{r})$, is given by

$$\phi_{cK}(\mathbf{r}) = \int_0^1 \mathrm{d}s\, \sigma_K(s) q_C(\mathbf{r}, s) q_C^*(\mathbf{r}, s) \tag{13b}$$

The total density of monomer $K$, $\phi_K(\mathbf{r})$, is a summation of the contribution from the homopolymers and the copolymers, $\phi_{hK}(\mathbf{r}) + \phi_{cK}(\mathbf{r})$. Once the density profiles are obtained, the SCFT free energy of the blends is given by

$$N_c F\beta/\rho_0 = -z_A Q_A - z_B Q_B - Q_C - \int \mathrm{d}\mathbf{r}(\chi N_c \phi_A \phi_B + \xi) \tag{14}$$

For the homogeneous phase, the fields, $w_K$, are constant in space. In this case the SCFT equations can be solved exactly, which gives a simple expression of the free energy density

$$\frac{N_c F\beta}{\rho_0 V} = \sum_K \frac{\phi_{hK}}{\alpha_K} \ln\left(\frac{\phi_{hK}}{\alpha_K} - 1\right) + \phi_C \ln \phi_C + \chi N_C \phi_A \phi_B - \sum_K \frac{\beta \mu_K \phi_{hK}}{\alpha_K} \tag{15}$$

This expression corresponds to the usual Flory−Huggins theory.[22]

For inhomogeneous phases, the SCFT equations, eqs 11−13, must be solved using numerical techniques. In the previous study of Jiang et al., the SCFT equations are solved using the reciprocal-space method.[52] The reciprocal-space method is particularly useful for the construction of phase diagrams containing complex ordered phases. In the present study, the polymer blends are assumed to be symmetric; therefore, the only ordered phase is the lamellar phase. In this case the problem is practically one-dimensional. We employ the split-step Fourier method introduced by Tzeremes et al. in our study.[56] Specifically, the modified diffusion equations are solved in a unit cell divided into 256 points. The contour length of the gradient copolymer chains is discretized into 256 intervals, as has been used in the RPA calculation. This value of intervals is chosen because Jiang et al. previously have shown that the free energy is insensitive to the number of intervals if $X > 200$.

## Results and Discussion

**Critical Lines.** The critical lines for different gradient copolymer/homopolymer blends can be obtained using the RPA described earlier. The results for symmetric blends ($\phi_{hA} = \phi_{hB}$, $\alpha_A = \alpha_B = 0.5$) with six types of gradient copolymers are shown in Figure 2. Specifically, the critical lines for the uniform distributed, diblock, and linear gradient copolymers are given in Figure 2a, whereas those for three tanh gradient copolymers with $\lambda$ equals 3, 5, and 10 are given in Figure 2b. For blends with uniform gradient copolymers, the critical line, specified by a critical incompatibility $\chi N_c = 2/\alpha(1 - \phi_c)$, is known as the Scott line.[59] At the Scott line, a homogeneous phase undergoes continuous liquid−liquid separation into two homopolymer-rich phases. For blends containing nonuniform gradient copolymers, the system may undergo microscopic phase separation. As the copolymer content is increased, the critical lines for diblock, linear, and tanh gradient copolymers follow the Scott line at the beginning and then depart from the Scott line at their corresponding Lifshitz points. Before and after the Lifshitz point, the nature of the phase separation changes from macroscopic to microscopic. The position of the LPs depends on the type of gradient copolymers. According to our numerical results, the LP for the blends containing diblock copolymers is determined at $(\phi_c)_L = 0.333$ and $(\chi N_c)_L = 5.991$, in agreement with earlier analytical results of Broseta and Fredrickson ($(\phi_c)_L = 1/3$ and $(\chi N_c)_L = 6$).[22] The LP for blends containing linear gradient copolymers is found to be at $(\phi_c)_L = 0.552$, $(\chi N_c)_L = 8.934$, whereas LP's for blends containing the three gradient

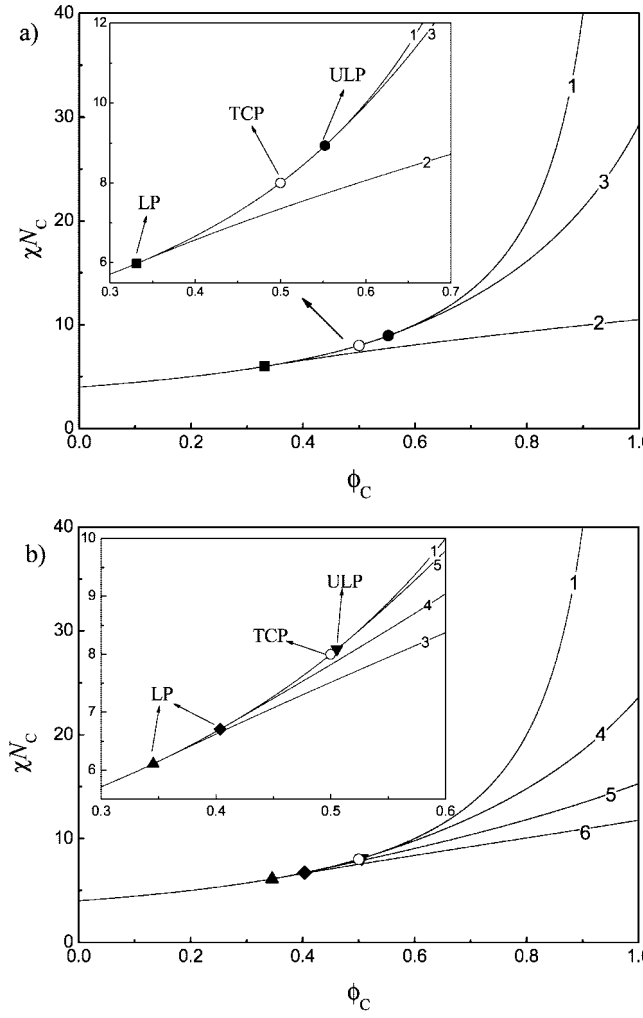


**Figure 2.** Critical lines of symmetric ternary blends for six types of gradient copolymers at $\alpha = 0.5$. Lines 1−7 correspond to uniform, diblock, linear and tanh ($\lambda = 3$, 5, and 10) gradient copolymers, respectively. The regions surrounding the Lifshitz points are enlarged in the inset. LP, TCP, and ULP indicate physical Lifshitz point, tricritical point, and unphysical Lifshitz point, respectively.

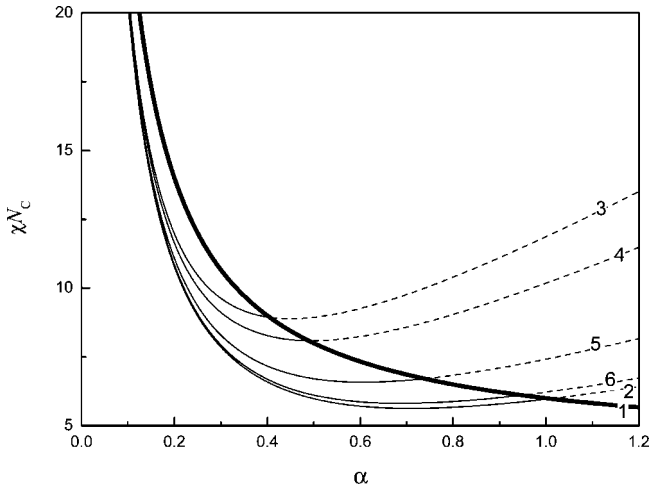


**Figure 3.** Critical incompatibility as a function of α. The thicker line, line 1, is the tricritical incompatibility. Lines 2−6 are Lifshitz incompatibilities of blends with diblock, linear, and tanh ($\lambda = 3$, 5, and 10) gradient copolymers, respectively. The physical parts of Lifshitz incompatibility are indicated by solid lines, and the unphysical parts are indicated by dashed lines.

copolymers ($\lambda = 3$, 5, and 10) are at $(\phi_c)_L = 0.506$, 0.404, 0.346 and $(\chi N_c)_L = 8.089$, 6.709, 6.111, respectively. These results indicate that, when the gradient distribution becomes more gradual, more copolymer content and higher incompatibility are needed to form a microphase. Furthermore, after passing the Lifshitz points, the critical lines for the different gradient copolymers deviate from each other and finally reach the critical points of pure gradient copolymers ($\phi_c = 1$) at $(\chi N_c)_c = 10.495$, 29.550, 23.611, 15.286, and 11.755 for diblock, linear, and the three tanh gradient copolymers, respectively. These values of the order−disorder transition (ODT) are in agreement with previously reported values.[51,52,54]

It should be noticed that, although the mean-field LPs for blends with different gradient copolymers can be calculated from RPA, only those ones located below the tricritical point (TCP) can be physically realizable.[22] The tricritical point corresponds to the position on the Scott line at which the blend starts to separate into three coexisting disordered phases (two homopolymer-rich and one copolymer-rich). The critical incompatibility of the TCP, $(\chi N_c)_{TCP} = 4 + 2/\alpha$, is easily obtained from the free energy of the homogeneous phase. If the LP is below the TCP, the appearance of three liquid phases is precluded by microphase separation; therefore, the LP could be physically realizable. On the other hand, if the LP is above the TCP, a three-phase region forms prior to the formation of the microphase, leading to an unphysical Lifshitz point (ULP). As illustrated in Figure 2, the nature of the LP depends on the steepness of gradient distribution. For $\alpha = 0.5$, the LPs of diblock and two tanh ($\lambda = 5$, 10) gradient copolymers are physical, whereas the LPs of the linear and tanh ($\lambda = 3$) gradient copolymers become unphysical. Thus, for the same relative chain length, LP can change gradually from physical to unphysical when the chain gradient becomes more gradual.

The nature of the Lifshitz point also depends on the relative chain lengths of the homopolymers and copolymers. It has been argued previously that short homopolymers can penetrate into the copolymer layers, therefore promoting microphase separation at lower incompatibility. On the other hand, owing to the loss of configuration entropy, long homopolymer chains cannot swell short block copolymers, leading to the disruption of the periodic structure and the formation of a disordered copolymer-rich phase. Figure 3 shows the relationship between the critical incompatibilities of LP, $(\chi N_c)_L$, and the relative chain length, α, for the different gradient copolymers. The critical incompatibility of the TCP, $(\chi N_c)_{TCP}$, is also shown for comparison. The necessary condition to make the LP physical is given by $(\chi N_c)_L < (\chi N_c)_{TCP}$. Our results show that the LP of diblock copolymer is physical when $\alpha < 1$, in agreement with the previous result by Broseta and Fredrickson.[22] The critical value of α for the linear gradient copolymer is limited to 0.4, whereas the critical values of α for the three tanh gradient copolymers ($\lambda = 3$, 5, and 10) are 0.49, 0.73, and 0.95, respectively. Therefore, when the gradient distribution changes from a steep profile (e.g., diblock) to a gradual profile (e.g., linear gradient), longer copolymer chains are needed to ensure that the Lifshitz point is physical.

From the above discussion on the critical lines of symmetric homopolymer/gradient copolymer blends, it can be concluded that it is more difficult for blends with gradual gradient copolymer to form microphases and to maintain a physical Lifshitz point. This tendency can be attributed to the increased miscibility of different components. For copolymers with gradual gradient distributions (e.g., linear gradient), segments become similar in composition, which makes them compatible with each other. As a result, the driving force for microscopic phase separation is reduced. The periodic structure found at the lower incompatibility for blends containing diblock copolymers can only occur at a higher incompatibility for blends containing gradual gradient copolymers. In the next section the free energy of inhomogeneous phases is computed using SCFT. Phase diagrams of the blends are constructed. It will be seen that the critical line determines the boundary of homogeneous and inhomogeneous regions. In addition, the relative positions of the LP and TCP can greatly influence the shape of phase diagram.

Before presenting the phase diagrams of the homopolymer/gradient copolymer blends, it is appropriate to comment on the applicability of the theoretical results to experimental observations. In the current investigation, the critical line and LP are obtained using random phase approximation, and the phase diagrams are calculated using the self-consistent mean-field theory. Therefore, the critical line, Lifshitz point, and phase diagrams presented here are obtained within the mean-field approximation, in which thermal fluctuations are ignored. On the other hand, it is well-known that thermal fluctuations will modify the mean-field behavior, sometime even qualitatively. Therefore, experimental observations do not adhere to the mean-field theory strictly. For the case of diblock copolymer melts, the effect of thermal fluctuations has been studied by Fredrickson and Helfand[60] using a framework developed by Brazovskii.[61] For symmetric diblock copolymers, they showed that thermal fluctuations change the nature of the order−disorder transition from second order within the mean-field theory to a weakly first-order transition. For the case of diblock copolymer/homopolymer blends, Kielhorn and Muthukumar have investigated the fluctuation effects at the weak segregation region using a one-loop self-consistent approximation,[62] which is a generalization of the Brazovskii theory.[61] Kielhorn and Muthukumar predicted that composition fluctuations change all the second-order mean-field microphase separation transitions to first-order ones, and the mean-field LP is destroyed by the composition fluctuations. These predictions were confirmed in a later experiment using small-angle neutron scattering.[63] Another example of thermal fluctuation effect is that, in the case of symmetric homopolymer/diblock copolymer blends, the unbinding transition line starting from the Lifshitz point is observed to become a channel of bicontinuous microemulsion region.[7−9] Despite these reservations, mean-field results, including the critical line, LP, and phase diagrams, on the phase behavior of polymer blends provide useful information about

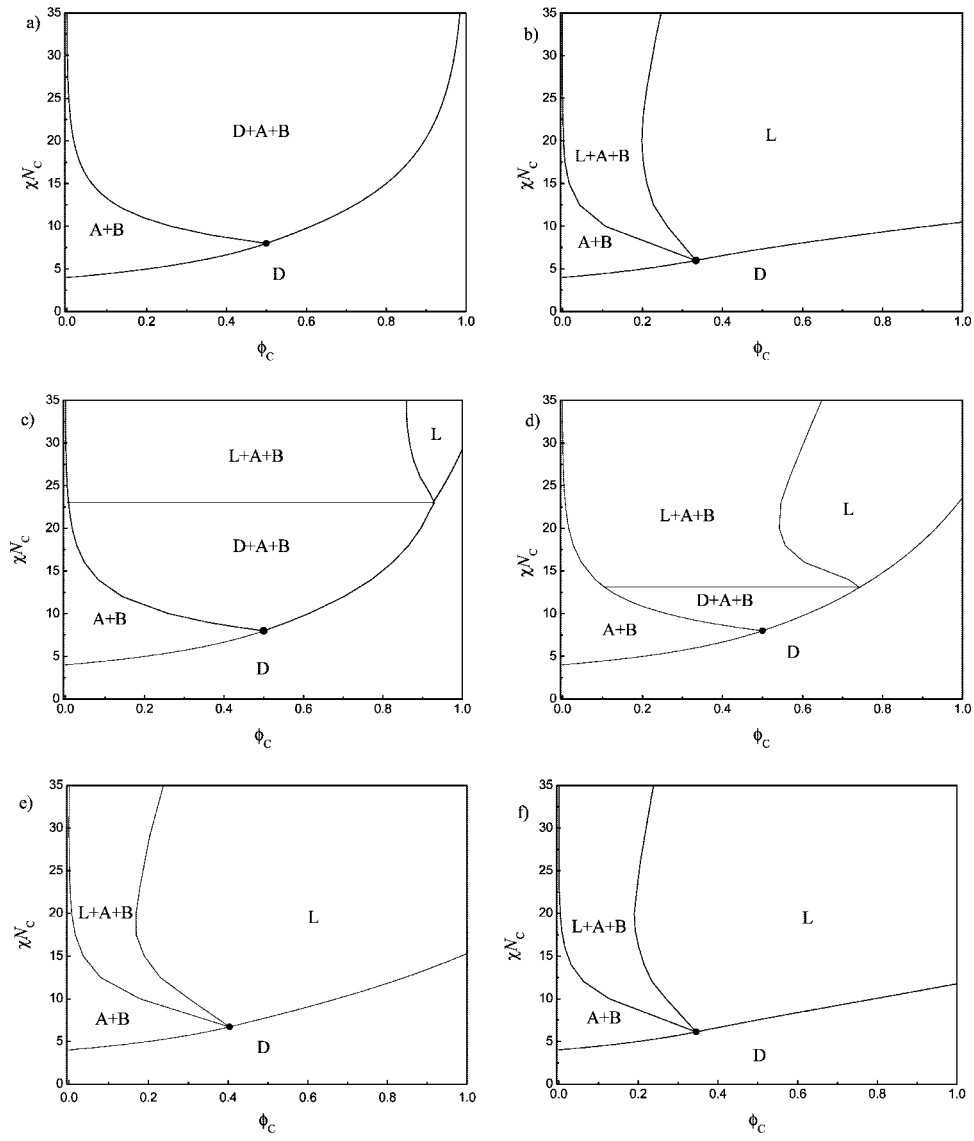


**Figure 4.** Phase diagrams of symmetric A/B/A-*g*-B blends. Parts a−f correspond to the blends with uniform, diblock, linear, and tanh ($\lambda$ = 3, 5, and 10) gradient copolymers, respectively. The different phase regions are homogeneous disordered phase "D", two homopolymer-rich coexisting phases "A + B", and lamellar phase "L".

the overall phase behavior of the system. For example, given the observation that the channel of the bicontinuous microemulsion phase follows closely the mean-field unbinding transition line, the mean-field phase diagrams can be used to design polymer blends for polymeric bicontinuous microemulsions. Furthermore, mean-field phase diagrams become accurate when the system is far away from the critical line.

**Phase Diagrams.** Phase diagrams along the isopleths ($\phi_{hA} = \phi_{hB}$) for symmetric blends of A and B homopolymers with six types of gradient copolymers are given in Figure 4. In all cases, the chain lengths of the homopolymers (A and B) are kept the same, and the chain length ratio of the homopolymers to the copolymers is kept at 0.5. With this choice of the parameters, the phase behavior of the blends is determined by three factors: the incompatibility ($\chi N_c$), the copolymer volume fraction ($\phi_c$), and the gradient distribution. Since the system is symmetric, it is expected that the only ordered phase in these systems is the lamellar phase.

The phase diagram for the blend containing uniform copolymers exhibits three regions. Below a tricritical point ($(\chi N_c)_{TCP} = 8$, $(\phi_c)_{TCP} = 0.5$), the homogeneous blend separates continuously into two homopolymer-rich phases, A + B, at the Scott line. Above the tricritical point, there is a large three-phase region. In this region, the blend undergoes first-order phase separation into two homopolymer-rich phases (A + B) and one copolymer-rich phase (D). Because of the appearance of the microphase, the shape of the phase diagram changes significantly when diblock copolymers are employed in the blends. As illustrated in Figure 4b, the phase diagram is divided into four regions around the Lifshitz point located at $(\chi N_c)_{LP} = 5.991$ and $(\phi_c)_{LP} = 0.333$. Below the Lifshitz point, the homogeneous blend undergoes macrophase separation into two homopolymer-rich phases (A + B) at the Scott line. A microscopically ordered lamellar phase (L) appears above the Lifshitz point. The L phase can be swollen by homopolymers up to 0.8 in volume fraction. When the lamellar phase becomes saturated with absorbed homopolymers, extra homopolymers are expelled from the copolymer matrix, forming two homopolymer-rich phases (A + B) in coexistence with the L phase. In a previous study, Janert and Schick suggested that the transition from the L phase to the A + B phase is a continuous unbinding transition.[28] In a related study, Naughton and Matsen identified this transition as a first-order one, but the free energy difference between the L and A + B phases is extremely small.[27] In our calculations, this transition is confirmed to be a first-

order one when an accuracy of $10^{-10}k_BT$ per molecule is used for the free energy.

There are five regions in the phase diagram for blends containing linear gradient copolymers, as shown in Figure 4c. As mentioned in previous section, in this case the Lifshitz point is precluded by the tricritical point, leading to a coexistence region of A + B and D at $(\chi N_c)_{TCP} < \chi N_c < (\chi N_c)_M = 23.06$, where $(\chi N_c)_M$ is the critical incompatibility for the microphase formation. It should be noted that the unphysical Lifshitz point is located inside this coexistence region. As a result, the appearance of the ordered L phase is precluded by the disordered D phase. An ordered microphase appears when the incompatibility is large enough, $\chi NC > (\chi N_c)_M$. At $(\chi N_c)_M$, four phases, A + B, D, and L coexist, and the D phase transfers to the L phase continuously. The L phase region is very small, indicating a poor ability of the lamellae formed by the linear gradient copolymers to swell homopolymers.

The phase diagrams of blends with three tanh gradient copolymers ($\lambda = 3$, 5, and 10) are shown in parts d, e, and f of Figure 4, respectively. For $\lambda = 3$, the shape of the phase diagram is similar to that of the linear gradient copolymers because the Lifshitz point in the present system is also unphysical. However, compared to the linear gradient copolymer case, the D phase in the tanh gradient copolymer blends with $\lambda = 3$ disappears at a lower incompatibility, $(\chi N_c)_M = 13.11$. Furthermore, the gradient copolymers can adsorb up to 50% homopolymers, which is much more than the 20% for the case of the linear gradient copolymers. Although there are big differences in gradient profiles between the tanh gradient copolymers with $\lambda = 5$, 10 and the diblock copolymers (Figure 1), it is surprising that their phase diagrams are almost identical (compare Figure 4e,f to Figure 4b). Since the Lifshitz points in these three systems are physical, these phase diagrams all exhibit four phase regions containing a large L phase region.

The phase diagrams given in Figure 4 demonstrate clearly that a different gradient distribution leads to very different phase behavior for blends containing gradient copolymers. As the gradient distribution becomes steeper (from uniform to diblock), the Lifshitz point of the blends changes from physical to unphysical. If the Lifshitz point is unphysical, the phase diagram always contains a disordered A + B + D coexistence region below the L phase. In this case the gradient copolymers behave almost as random copolymers. When the gradient distribution becomes steeper, the region of the A + B + D phase becomes smaller and the D phase disappears at lower incompatibility. In addition, the ability of copolymers to absorb homopolymers changes appreciably with gradient steepness. On the other hand, if the Lifshitz point is physical, the D phase disappears. An ordered L phase occupies a larger region in the phase diagram. The ability to absorb homopolymers into the copolymer layers is increased greatly in the physical LP case than the unphysical LP case. It is found that the size of the L phase region is not sensitive to the details of the chain gradient, indicating that copolymers with certain gradient steepness have almost the same ability to swell homopolymer. Moreover, a major role of the copolymers is to serve as compatibilizers of immiscible homopolymers. The phase diagrams in Figure 4 show that more copolymer chains can be dissolved into the homopolymer-rich phases (A + B phases) when smooth gradient copolymers are employed as compatibilizer.

**Structure of the Ordered Microphase.** The self-consistent-field theory can be used to calculate the density profile of each component and the spatial distribution of chain segments when the system forms microphases. Because many of physical properties of a blend are related to the monomer distributions, it is useful to compute these properties. In this section, a diblock copolymer and two tanh gradient copolymers ($\lambda = 3$, 5) are employed to illustrate the effects of the gradient distribution on the monomer profiles. In all cases $\phi_c$ and $\chi N_c$ are fixed at 0.60 and 29, respectively, in the blends. Under these conditions, all three blends form a lamellar phase according to the phase diagrams shown in Figure 4.

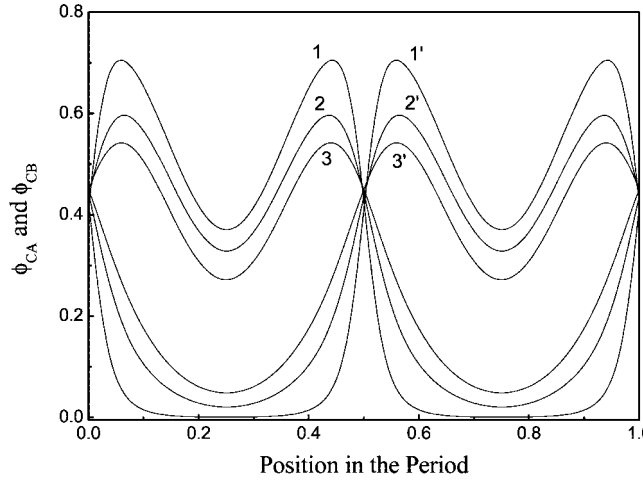


**Figure 5.** Density profiles of gradient copolymers. Lines 1, 2, and 3 (1′, 2′, and 3′) are the densities of A (B)monomers in diblock, tanh gradient ($\lambda = 5$, 3) copolymers.

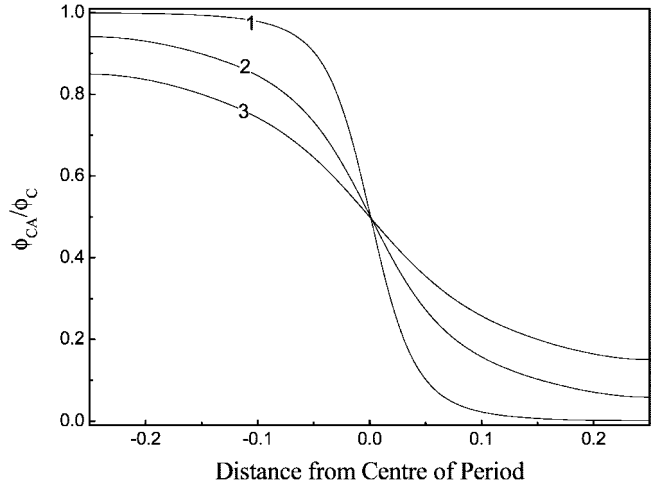


**Figure 6.** Spatial profile of A monomers. Lines 1, 2, and 3 denote the cases of diblock and tanh gradient ($\lambda = 5$, 3) copolymers, respectively.

The lamellar phase corresponds to a one-dimensional periodic structure. Within one period, the structure can be divided into sequential arrangements of homopolymer and copolymer layers that are rich in A and B, respectively. The structures of the copolymer layers of the three blends are quite different, as seen in the density profiles (Figure 5). For the blend containing the diblock copolymers, the density of the B monomers decreases rapidly when entering into the A-rich layer. On the contrary, the B monomer density decreases slowly and extends deep inside the A-rich layer for the blends containing the tanh gradient copolymers. Figure 6 shows the fraction of A monomers from the copolymers. For the case of diblock copolymers, the copolymer layer is broad and composed of mostly of one type of monomers. The interface between two adjacent A and B copolymer layers is narrow. For the case of tanh gradient copolymers, the copolymer layer becomes narrow and contains both types of monomers. In addition, the interface region becomes broader and more diffuse as the chain gradient becomes smoother. Moreover, the copolymer chains are arranged more randomly in the interface region when the tanh gradient

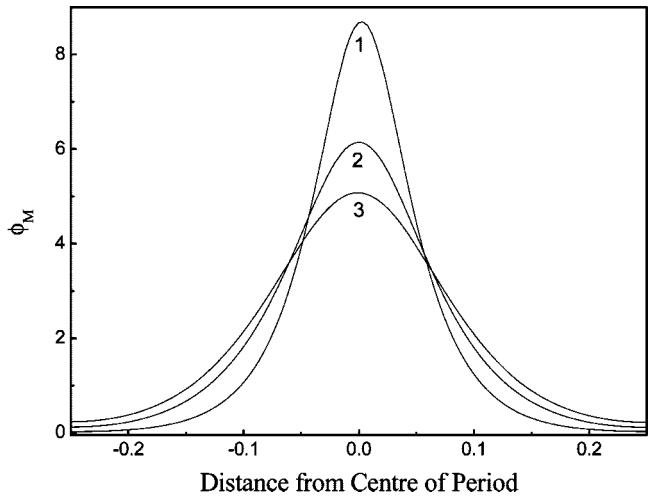


**Figure 7.** Spatial distribution of the middle section of copolymers. Lines 1, 2, and 3 correspond to diblock and tanh gradient ($\lambda$ = 3, 5) copolymers, respectively.

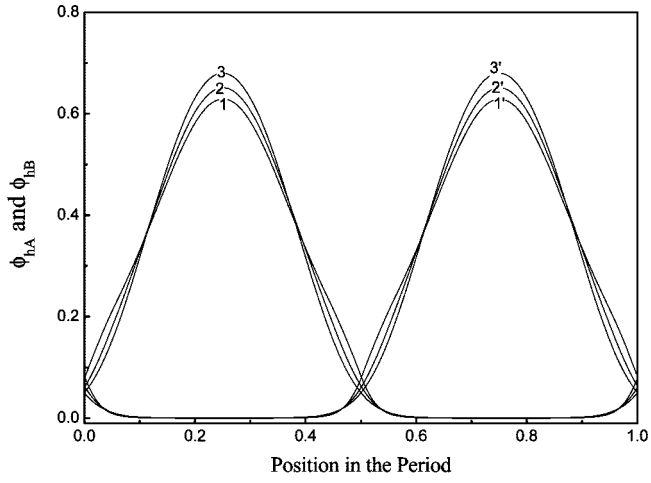


**Figure 8.** Density profiles of homopolymers. Lines 1, 2, and 3 (1′, 2′, and 3′) correspond to the densities of A (B) homopolymers for blends containing the diblock and tanh gradient ($\lambda$ = 3, 5) copolymers.

copolymer is used instead of the diblock copolymer. Figure 7 illustrates the spatial distribution of the middle section of the gradient copolymers. For the case of the diblock copolymers, the middle section is localized in a narrow region near the interface. On the other hand, the corresponding distribution of the middle blocks becomes much wider when the gradient distribution becomes more gradual. The width of the peak at half-height of the distribution occupies as much as 20% of the period for the tanh gradient copolymers with $\lambda = 3$ as compared with 10% for the case of diblock copolymers. This diffusive arrangement of the copolymers at the interfacial region is a characteristic of gradient copolymers.

The type of gradient copolymer in the blend also affects the density profile of the homopolymers, as shown in Figure 8. As the gradient distribution becomes more gradual, the homopolymer fraction in the homopolymer layer increases, whereas the homopolymer fraction in the copolymer layer decreases. It can be seen from Figure 8 that, compared to the case of tanh gradient copolymers with $\lambda = 3$, about 15% more homopolymers prefer to be inside the copolymer layer for the diblock copolymer case. In addition, steeper gradient copolymers lead to a larger penetration of the homopolymer into the copolymer layer.

The structure of the copolymer and homopolymer layers and the interfaces between them for blends with different types of

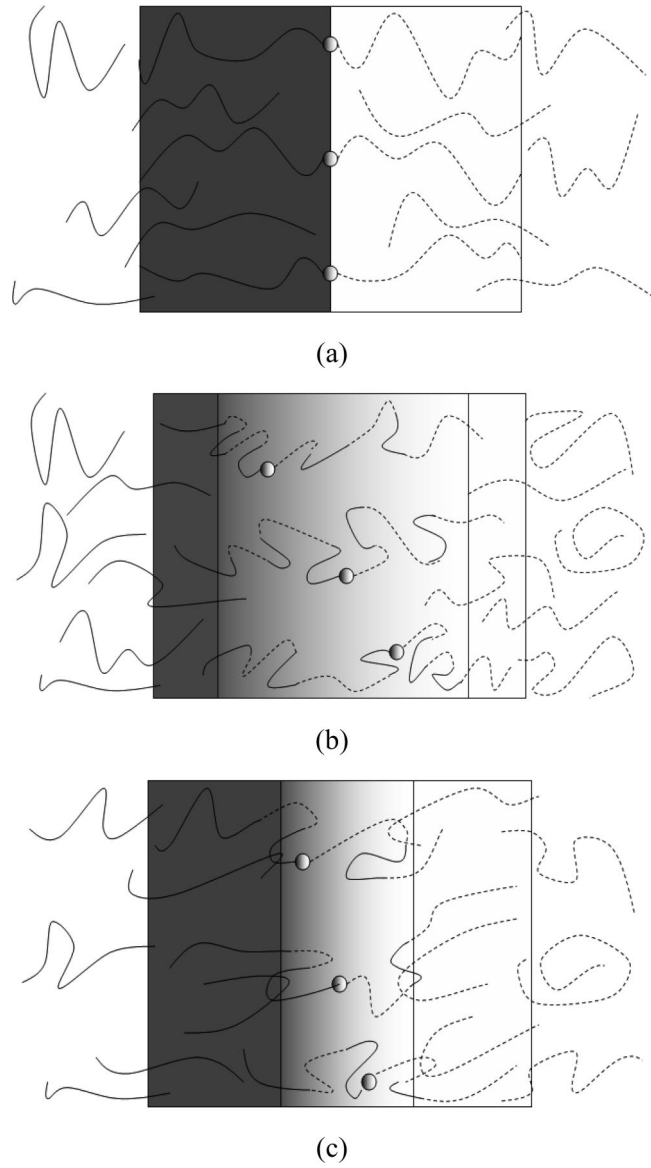


**Figure 9.** Schematic illustration of microstructures formed by blends involving copolymers with (a) steep (b) smooth and (c) intermediate gradient distributions. Circle denotes the position of the middle section in gradient copolymer chains. Solid and dashed lines denote the chain sections composed of A and B, respectively. The darkness of the background illustrates the A monomer fraction in the copolymer layer.

gradient copolymers are given in Figure 9. For the copolymers with a steep gradient distribution, e.g., diblock copolymers or tanh gradient copolymers with $\lambda$ = 10, the arrangement of copolymer chains is quite ordered with its middle section localized near the center plane between the A−B layers. A large part of the homopolymers is found inside the copolymer layer, a portion of which extends almost to the A−B interface. This structure greatly strengthens the connection between the homopolymer and copolymer layers and can explain the strong ability for steep gradient copolymers to absorb homopolymers into the interfacial layers. For the more gradual gradient copolymers, e.g., linear gradient copolymers or tanh gradient copolymers with $\lambda = 3$, the A−B interface becomes broad and diffuse, in which the copolymers are distributed randomly. In addition, the copolymer layers are narrow, which prevent further penetration of the homopolymers due to unfavorable interaction between the different types of monomers. Therefore, the homopolymers tend to be expelled from the interface between the copolymer layers. In this case the ability for the copolymer

layers to absorb homopolymers is noticeably reduced and the interface between the homopolymer and copolymer layers would be weakened.

In the case of copolymers with intermediate chain gradients, e.g., tanh gradient copolymer with $\lambda = 5$, the L phase cannot absorb as large an amount of homopolymer as it did in the case where diblock copolymers and long homopolymer chains are used. However, its ability to adsorb short homopolymer chains is as strong as the L phase of diblock copolymers because its copolymer layers maintain similar width as compared to the size of the short homopolymers. The deep penetration of homopolymer chains also increases the probability of them entering the interfacial region between the copolymer layers. Since most synthesized gradient copolymers have a multiblock feature, the sections of copolymer chains in the interfacial region is expected to form either a back and forth or zigzag pattern, similar to the conclusion of Dai et al.,[64] or a nearly random coil as predicted by Noolandi and Shi.[65] Both of these two models bring about self-stitching loops, which can be entangled by homopolymer chains as depicted in Figure 9c. This loop entanglement could greatly reinforce adhesion at the interfaces.

The above analysis of the microphase structures can explain some of the phase behavior observed in previous sections. Furthermore, it also provides guidance for the design of effective compatibilizers. An effective compatibilizer should segregate to the homopolymer/homopolymer interfaces. In addition, only a small amount of compatibilier should be sufficient to reinforce the adhesion of interfaces. Previously, diblock copolymers were considered to be the best choice since they can organize themselves at the interfaces with two blocks entangled by homopolymers. In practice, diblock copolymers have several disadvantages as compatibilizers, such as high cost and a strong tendency to form micelles. The formation of micelles will compete with the segregation of block copolymers to the interfaces. It has been proposed that random copolymers could be used to reinforce the interfaces in a homopolymer/copolymer/homopolymer sandwich structure specially prepared by layer-by-layer spin-casting. The loop structures can be formed at the interface, which could increase entanglements between copolymer and homopolymer chains. But in a practical blending process, random copolymers have little effect as compatibilizers due to the lack of a strong driving force to segregate to interfaces. Through carefully design of the composition profile, some types of gradient copolymers may combine the advantages of diblock copolymers and random copolymers. In previous publications, Shull[53] and Wong et al.[66] concluded that gradual gradient copolymers are more difficult to form micelles than diblock copolymers. Since the two ends of gradient copolymers are nearly pure A or B type, they can be anchored by entanglement with adjacent homopolymers, similar to what would occur for diblock copolymers. At the same time the middle blocks of the gradient copolymers could bring about a disordered region, where the chain segments behave almost like a random copolymer and form self-stitching loops. The homopolymers can be further entangled by these loops, resulting in a reinforced interface between the A and B homopolymers. Experimentally, Kim et al.[47,48] have reported that their synthesized gradient copolymers are effective as compatibilizers, in agreement with the physical model proposed from our SCFT results.

Copolymers can also serve as a template for nanostructured blends, whose application might be important in future polymer industries.[10] The new blends will require integration of multiple functions in the nanometer scale. The abrupt compositional change at the interface in diblock copolymers may lead to sharp switching of properties, whereas the gradual transition in the interface structure of a gradient copolymer, as evident in Figure 9, may lead to special thermal, mechanical, and transport properties. The broad glass transition temperatures of gradient copolymers reported both by Kim et al.[48] and Sun et al.[44] are a typical reflection of the great potential of these kinds of materials. Depending on the requirements of the application, the properties of blends can be fine-tuned by adjustment of the copolymer gradient and the blend recipe.

## Conclusions

In this paper, a multiblock model is employed to describe the composition profiles of gradient copolymers. The model system is studied using random phase approximation analysis and self-consistent-field theory. Phase diagrams of symmetric polymer blends with a series of gradient copolymers are constructed, which could be used to help in the design of polymer blends. The effects of the gradient distribution on the phase behavior of ternary homopolymer/gradient copolymer blends are systematically studied. From our theoretical studies the following conclusions are reached:

The composition profiles of gradient copolymers have a significant effect on the critical behavior of the blends. As the gradient distribution changes from steep to gradual, the formation of ordered microphases becomes more difficult since the gradient copolymers gradually change from block copolymers to random polymers. The Lifshitz point is also shifted to higher values of the critical copolymer content and the critical incompatibility. In addition, the nature of the Lifshitz point changes from physical to unphysical. Furthermore, much longer copolymer chains are needed to maintain the physical nature of the Lifshitz point for gradual gradient distributions than for steep ones.

The composition profiles of gradient copolymers greatly affect the phase diagram of the blends. When the Lifshitz points are physical, the blends always exhibit four phases: disordered phase, A + B, L, and L + A + B. The lamellar phases occupy a large region in the phase diagrams, showing the strong ability of these types of gradient copolymers to absorb the homopolymers. On the other hand, there are five phases in the phase diagrams of blends when the Lifshitz points are unphysical. A disordered coexisting A + B + C phase region exists below the L phase. The gradient copolymers with steep composition profiles increase the region of L phase and reduce the region of coexisting A + B + D phases. Moreover, more copolymer chains can be dissolved into the homopolymer rich phases (A + B phases) when gradual gradient copolymers are employed as a compatibilizer.

The microphase structures of the blends, including the broadness and distribution of copolymer layers, the width of interface region, and the distribution of homopolymers, also depend on the gradient distributions. Gradual gradients make the copolymer layers narrow and randomly distributed, broaden the diffusion interface region where the copolymer chains arrange randomly, and prevent the penetration of homopolymer chains to the copolymer layers.

The chain structure of gradient copolymers provides a flexible lever to optimize the morphology and other properties of blends. By designing the composition profiles of copolymer chains, the adhesion between two homopolymer layers could be reinforced and other interfacial properties of blends could also be fine-tuned.

**Acknowledgment.** We acknowledge financial support from The National Science Foundation of China (NSFC Grant #20774087) and the Natural Science and Engineering Research Council (NSERC) of Canada. Rui Wang gratefully acknowledges the hospitality of McMaster University, where this work was carried out during a 3-month visit. We thank Dr. Robert A. Wickham for

many helpful discussions on gradient copolymers and for a thorough reading of the manuscript.

## References and Notes


(1) Paul, D. R.; Newman, S. *Polymer Blends*; Academic Press: New York, 1978.
(2) Utracki, L. A. *Polymer Alloys and Blends: Thermodynamics and Rheology*; Hanser Pub: New York, 1989.
(3) Milner, S. T. *Mater. Res. Soc. Bull.* **1997**, *22*, 38.
(4) Koning, C.; Van Duin, M.; Pagnoulle, C.; Jerome, R. *Prog. Polym. Sci.* **1998**, *23*, 707.
(5) Creton, C.; Kramer, E. J.; Brown, H. R.; Hui, C. Y. *Adv. Polym. Sci.* **2002**, *156*, 53.
(6) Koizumi, S.; Hasegawa, H.; Hashimoto, T. *Macromolecules* **1994**, *27*, 6532.
(7) Bates, F. S.; Maurer, W. W.; Lodge, T. P.; Schulz, M. F.; Matsen, M. W.; Almdal, K.; Mortensen, K. *Phys. Rev. Lett* **1995**, *75*, 4429.
(8) Bates, F. S.; Maurer, W. W.; Lipic, P. M.; Hillmyer, M. A.; Almdal, K.; Mortensen, K.; Fredrickson, G. H.; Lodge, T. P. *Phys. Rev. Lett.* **1997**, *79*, 849.
(9) Hillmyer, M. A.; Maurer, W. W.; Lodge, T. P.; Bates, F. S.; Almdal, K. *J. Phys. Chem. B* **1999**, *103*, 4814.
(10) Ruzette, A.; Leibler, L. *Nat. Mater.* **2005**, *4*, 19.
(11) Matsen, M. W. *J. Phys.: Condens. Matter* **2002**, *14*, 21.
(12) Fredrickson, G. H. *The Equilibrium Theory of Inhomogeneous Polymers*; Oxford University Press: Oxford, 2006.
(13) Leibler, L. *Macromolecules* **1980**, *13*, 1602.
(14) Helfand, E. *J. Chem. Phys.* **1975**, *62*, 999.
(15) Helfand, E.; Wasserman, Z. R. *Macromolecules* **1976**, *9*, 879.
(16) Semenov, A. N. *Macromolecules* **1992**, *25*, 4976.
(17) Matsen, M. W.; Schick, M. *Phys. Rev. Lett.* **1994**, *72*, 2660.
(18) Matsen, M. W.; Schick, M. *Macromolecules* **1994**, *27*, 7157.
(19) Matsen, M. W.; Bates, F. S. *Macromolecules* **1996**, *29*, 1091.
(20) Fredrickson, G. H.; Ganesan, V.; Drolet, F. *Macromolecules* **2002**, *35*, 16.
(21) Guo, Z.; Zhang, G.; Qiu, F.; Zhang, H.; Yang, Y.; Shi, A. C. *Phys. Rev. Lett.* **2008**, *101*, 028301.
(22) Broseta, D.; Fredrickson, G. H. *J. Chem. Phys.* **1990**, *93*, 2927.
(23) A Lifshtz point (LP) occurs in a physical system in which the ordered phase changes from a spatially uniform (two-phase) to a spatially modulated (lamella) structure. The LP was first studied in the content of magnetic systems in: Hornreich, R. M.; Luban, M.; Shtrikman, S. *Phys. Rev. Lett.* **1975**, *35*, 1678.
(24) Muller, M.; Schick, M. *J. Chem. Phys.* **1996**, *105*, 8885.
(25) Matsen, M. W. *Phys. Rev. Lett.* **1995**, *74*, 4225.
(26) Matsen, M. W. *Macromolecules* **1995**, *28*, 5765.
(27) Naughton, J. R.; Matsen, M. W. *Macromolecules* **2002**, *35*, 5688.
(28) Janert, P. K.; Schick, M. J. *Macromolecules* **1997**, *30*, 3916.
(29) Janert, P. K.; Schick, M. J. *Macromolecules* **1997**, *30*, 137.
(30) Janert, P. K.; Schick, M. J. *Macromolecules* **1998**, *31*, 1109.
(31) Duchs, D.; Ganesan, V.; Fredrickson, G. H.; Schmid, F. *Macromolecules* **2003**, *36*, 9237.
(32) Shull, K. R. *Macromolecules* **1993**, *26*, 2343.
(33) Matsen, M. W. *J. Chem. Phys.* **1999**, *110*, 4658.
(34) Thompson, R. B.; Matsen, M. W. *Phys. Rev. Lett.* **2000**, *85*, 670.
(35) Shull, K. R.; Kramer, E. J.; Hadziioannou, G.; Tang, W. *Macromolecules* **1990**, *23*, 4780.
(36) Lee, M. S.; Lodge, T. P.; Macosko, C. W. *J. Polym. Sci., Part B: Polym. Phys.* **1997**, *35*, 2835.
(37) Davis, K. A.; Matyjaszewski, K. *Adv. Polym. Sci.* **2002**, *159*, 1.
(38) Matyjaszewski, K.; Xia, J. H. *Chem. Rev.* **2001**, *101*, 2921.
(39) Matyjaszewski, K. *Prog. Polym. Sci.* **2005**, *30*, 858.
(40) Ziegler, M. J.; Matyjaszewski, K. *Macromolecules* **2001**, *34*, 415.
(41) Matyjaszewski, K.; Ziegler, M. J.; Arehart, S. V.; Greszta, D.; Pakula, T. *J. Phys. Org. Chem.* **2000**, *13*, 775.
(42) Wang, R.; Luo, Y.; Li, B.; Zhu, S. *AIChE J.* **2007**, *53*, 174.
(43) Sun, X.; Luo, Y.; Wang, R.; Liu, B.; Li, B.; Zhu, S. *Macromolecules* **2007**, *40*, 849.
(44) Sun, X.; Luo, Y.; Wang, R.; Li, B.; Zhu, S. *AIChE J.* **2008**, *54*, 1073.
(45) Wang, R.; Luo, Y.; Li, B.; Sun, X.; Zhu, S. *Macromol. Theory Simul.* **2006**, *15*, 356.
(46) Jouenne, S.; González-León, J. A.; Ruzette, A.; Lodefier, P.; Tencé-Girault, S.; Leibler, L. *Macromolecules* **2007**, *40*, 2423.
(47) Hodrokoukes, P.; Floudas, G.; Pispas, S.; Hadjichristidis, N. *Macromolecules* **2001**, *34*, 650.
(48) Kim, J.; Michelle, M. M.; Robert, W. S.; Dong, J. W.; John, M. T. *Macromolecules* **2006**, *39*, 6152.
(49) Kim, J.; Gray, M. K.; Zhou, H. Y.; Nguyen, S. T.; Torkelson, J. M. *Macromolecules* **2005**, *38*, 1037.
(50) Kim, J.; Zhou, H. Y.; Nguyen, S. T.; Torkelson, J. M. *Polymer* **2006**, *47*, 5799.
(51) Aksimentiev, A.; Holyst, R. *J. Chem. Phys.* **1999**, *111*, 2329.
(52) Lefebvre, M. D.; de la Cruz, M. O.; Shull, K. R. *Macromolecules* **2004**, *37*, 1118.
(53) Shull, K. R. *Macromolecules* **2002**, *35*, 8631.
(54) Jiang, R.; Jin, Q. H.; Li, B. H.; Ding, D. T.; Wickham, R. A.; Shi, A. C. *Macromolecules* **2008**, *41*, 5457.
(55) de Gennes, P. G. *Scaling Concept in Polymer Physics*; Cornell University Press: Ithaca, NY, 1979.
(56) Tzeremes, G.; Rasmussen, K. Ø.; Lookman, T.; Saxena, A. *Phys. Rev. E* **2002**, *65*, 041806.
(57) Li, W. H.; Wickham, R. A. *Macromolecules* **2006**, *39*, 8492.
(58) Odian, G. *Principle of Polymerization*; John Wiley & Sons: Hoboken, NJ, 2004.
(59) Scott, R. L. *J. Polym. Sci.* **1952**, *9*, 423.
(60) Fredrickson, G. H.; Helfand, E. *J. Chem. Phys.* **1987**, *87*, 697.
(61) Brasovskii, S. A. *Sov. Phys. JETP* **1975**, *61*, 85.
(62) Kielhorn, L.; Muthukumar, M. *J. Chem. Phys.* **1997**, *107*, 5588.
(63) (a) Schwahn, D. *Adv. Polym. Sci.* **2005**, *183*, 1. (b) Pipich, V.; Schwahn, D.; Willner, L. *Phys. Rev. Lett.* **2005**, *94*, 117801.
(64) Dai, C. A.; et al. *Phys. Rev. Lett.* **1994**, *73*, 2472.
(65) Noolandi, J.; Shi, A. C. *Phys. Rev. Lett.* **1995**, *74*, 2836.
(66) Wong, C. L. H.; Kim, J.; Roth, C. B.; Torkelson, J. M. *Macromolecules* **2007**, *40*, 5631.


MA801398A